Biometals (2019) 32:671–682
https://doi.org/10.1007/s10534-019-00204-5

Synthesis and antimicrobial activity of a phenanthroline-isoniazid hybrid ligand and its Ag^{+} and Mn^{2+} complexes

Muhib Ahmed · Denise Rooney · Malachy McCann · Michael Devereux · Brendan Twamley · Anna Clara Milesi Galdino · Leandro Stefano Sangenito · Lucieri Olegario Pereira Souza · Maria Cristina Lourenço · Karen Gomes · André Luis Souza dos Santos

Received: 24 April 2019 / Accepted: 14 June 2019 / Published online: 22 June 2019

Abstract Hydrazide ligand, (*Z*)-*N'*-(6-oxo-1,10-phenanthrolin-5(6H)-ylidene)isonicotinohydrazide, **1** forms from a 1:1 Schiff base condensation reaction between isoniazid (INH) and 1,10-phenanthroline-5,6-dione (phendione). Ag^{+} and Mn^{2+} complexes with 1:2 metal:ligand stoichiometry are prepared: $[Ag(\mathbf{1})_2]NO_3$, $[Ag(\mathbf{1})_2]BF_4$ and $[Mn(\mathbf{1})_2](NO_3)_2$. Polymeric $\{[Ag(\mathbf{1})(NO_3)]\}_n$ has 1:1 stoichiometry and forms upon infusion of CH_2Cl_2 into a DMSO solution of $[Ag(\mathbf{1})_2]NO_3$. $\{[Ag(\mathbf{1})(NO_3)]\}_n$ was structurally characterized using X-ray crystallography. Metal-free **1** and its 1:2 complexes exhibit very good, broad-spectrum antimicrobial activity and are not excessively toxic to mammalian cells (A549 lineage).

Keywords 1,10-Phenanthroline · Metal complexes · Antibacterial activity · Antibiotic resistance · Anti-tuberculosis activity

Introduction

Pathogenic bacteria, fungi, parasites and viruses can trigger sepsis, a condition whereby the body's response to infection induces tissue and organ dysfunction, leading to excessive morbidity and mortality. In both community and clinic settings septicaemia is estimated to affect over 30 million people annually and causes up to 6 million fatalities (WHO factsheet 2018). The World Health Assembly (WHA) (Seventh WHA 2018) and the World Health Organization (WHO) (WHO factsheet 2018) both acknowledge that more investment is required for research into finding

Electronic supplementary material The online version of this article (https://doi.org/10.1007/s10534-019-00204-5) contains supplementary material, which is available to authorized users.

M. Ahmed · D. Rooney (✉) · M. McCann
Department of Chemistry, Maynooth University, Maynooth, County Kildare, Ireland
e-mail: denise.rooney@mu.ie

M. Devereux
The Inorganic Pharmaceutical and Biomimetic Research Centre, Focas Research Institute, TU Dublin - City Campus, Kevin Street, Dublin 8, Ireland

B. Twamley
School of Chemistry Trinity College Dublin, University of Dublin, Dublin 2, Ireland

A. C. M. Galdino · L. S. Sangenito · L. O. P. Souza · A. L. S. dos Santos
Department of General Microbiology, Microbiology Institute Paulo de Góes, Federal University of Rio de Janeiro, Rio de Janeiro, Brazil

M. C. Lourenço · K. Gomes
Bacteriology Laboratory, Evandro Chagas Clinical Research Institute, Oswaldo Cruz Foundation, Rio de Janeiro, Brazil

new and cost-effective antimicrobials to overcome the major problem of drug resistance.

Since the 1950s, metal-free ligands and coordination complexes constituted by members of the 1,10-phenanthroline family of *N,N'*-chelating ligands have been shown to inhibit the growth of potentially harmful microorganisms (MacLeod 1952; Dwyer et al. 1957, 1969a, b; Shulman and Dwyer 1964; Butler et al. 1969, 1970; Cade et al. 1970; McCann et al. 2012a, b; Viganor et al. 2017; McCarron et al. 2018). Dwyer et al. (1969a, b) formulated and patented phenanthroline-containing therapeutics for topical application to humans, lower animals and plants in order to combat diseases induced by a wide variety of organisms. In 1970 in Melbourne, Australia, the results of two controlled clinical trials (Cade et al. 1970; Bulter et al. 1970) on patients suffering from topical infections due to fungi, bacteria and protozoa showed the highly beneficial effects of the topical application of formulations containing Mn^{2+}, Cu^{2+} and Ni^{2+} complexes of 3,4,7,8-tetramethyl-1,10-phenanthroline. Additionally, the metal complexes were non-toxic and it was reported in the trial involving the Mn^{2+} complexes (Cade et al. 1970) that microbial resistance did not develop.

In the current paper, we outline the synthesis of a new Schiff base ligand, **1**, derived by reacting the anti-tuberculosis drug, isoniazid (INH), with 1,10-phenanthroline-5,6-dione (phendione) (Scheme 1). Ag^{+} and Mn^{2+} complexes of **1** were also prepared and one of the Ag^{+} species was structurally characterised. Also presented are the results of in vitro growth inhibition tests against bacterial (*Mycobacterium tuberculosis*, *Staphylococcus aureus* and *Pseudomonas aeruginosa*) and fungal (*Candida albicans*) pathogens. Additionally, the cytotoxicity of **1** and its complexes towards lung epithelial A549 cells was assessed and selectivity index (SI) values established.

Materials and methods

All reagents used in chemical syntheses were commercially available (Sigma-Aldrich) and were used as supplied. Phendione was synthesised using a literature procedure (Zheng et al. 2010). All experiments involving Ag^{+} compounds were conducted in the absence of light and samples were stored in the dark. NMR (Nuclear Magnetic Resonance) spectra were recorded on a Bruker Avance spectrometer operating at 500 MHz for ^{1}H nucleus and 125 MHz for the ^{13}C nucleus. The probe temperature was maintained at 25 °C. Electrospray ionization (ESI) High Resolution Mass Spectrometry (HRMS) analyses were collected on an Agilent-L 1200 Series coupled to a 6210 Agilent Time-of-Flight (TOF) equipped with both a positive and negative electrospray source.

Infrared spectra were recorded as KBr discs in the region 4000–400 cm^{-1} on a Perkin-Elmer 100 series spectrometer. Elemental analyses (%CHN) were carried out using a FLASH EA 1112 Series Elemental Analyser with Eager 300 operating software. Magnetic moment measurements were taken at room temperature using a Johnson Matthey Magnetic Susceptibility Balance with $Hg[Co(SCN)_4]$ being used as the calibration standard.

X-ray structural analysis for crystals of $\{[Ag(\mathbf{1})(NO_3)]\}_n$ (Table 1) were performed on a Bruker APEX Duo CCD at 100(2) K with an Oxford Cobra cryostat, with the sample mounted on a MiTeGen microloop using Mo Kα radiation (λ = 0.71073 Å). Bruker APEX (Bruker 2015) software was used to collect and reduce data and determine the space group. Absorption corrections were applied using SADABS (Bruker 2014–2015). Structures were solved with the XT structure solution program (Sheldrick 2015) using Intrinsic Phasing and refined with the XL refinement package (Sheldrick

Scheme 1 Synthesis of ligand **1**

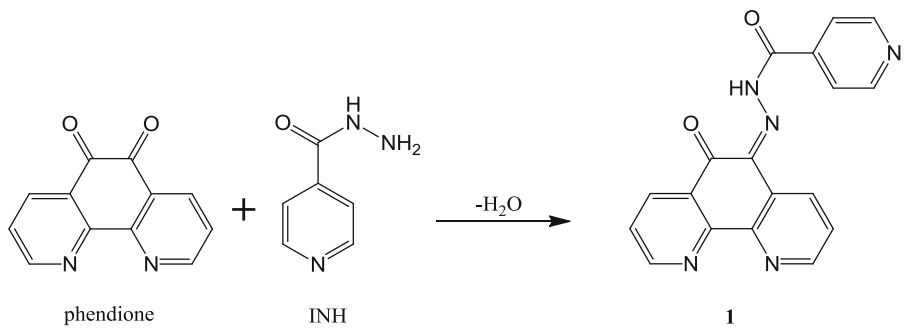

phendione INH **1**

Table 1 Crystal data and structure refinement details for $\{[Ag(\mathbf{1})(NO_3)]\}_n$

Identification code	$\{[Ag(\mathbf{1})(NO_3)]\}n$
Empirical formula	$C_{18}H_{11}AgN_6O_5$
Formula weight	499.20
Temperature (K)	100(2)
Wavelength (Å)	0.71073
Instrument	Bruker APEX DUO
Crystal system	Triclinic
Space group	P1
a (Å)	8.3219(15)
b (Å)	10.3830(18)
c (Å)	10.5249(19)
α (°)	73.092(2)
β (°)	80.063(3)
γ (°)	79.284(3)
Volume ($Å^3$)	848.1(3)
Z	2
ρ (calc. Mg/m^3)	1.955
μ (mm^{-1})	1.239
F(000)	496
Crystal size (mm^3)	0.13 × 0.12 × 0.05
Theta range for data collection (°)	2.039 to 27.186
Reflections collected	11367
Independent reflections	3790 [R(int) = 0.0621]
Max. and min. transmission	0.7455 and 0.6472
Data/restraints/parameters	3790/1/275
Goodness-of-fit on F^2	1.025
Final R indices [$I > 2\sigma(I)$]	R1 = 0.0419, wR2 = 0.0659
R indices (all data	R1 = 0.0685, wR2 = 0.0719
Largest diff. peak and hole (e $Å^{-3}$)	0.533 and − 0.875
CCDC No.	1907353

2008) using Least Squares minimisation in Olex2 (Dolomanov et al. 2009). All non-hydrogen atoms were refined anisotropically. Hydrogen atoms were assigned to calculated positions using a riding model with appropriately fixed isotropic thermal parameters. The amide hydrogen atom H9 was located and refined with restraints (DFIX).

Chemical synthesis

*(Z)-N′-(6-oxo-1,10-phenanthrolin-5(6H)-ylidene)isonicotinohydrazide (**1**)*

1,10-Phenanthroline-5,6-dione (phendione) (0.210 g, 1.000 mmol) was added to solution of isonicotinic acid hydrazide (isoniazid, (INH)) (0.137 g, 1.000 mmol) in EtOH (25 cm^3). *p*-Toluenesulfonic acid (10%, 0.02 g, 0.10 mmol) was added and the solution refluxed for 6 h. The resulting suspension was filtered whilst hot to remove a very small quantity of precipitated 1,10-phenanthroline-5,6-diol. The bright orange filtrate was allowed to stand in the dark overnight. Yellow needles of **1** were filtered off, washed with EtOH (3 × 10 cm^3) and air-dried.

Yield: 0.263 g, 79%. MP: 210–211 °C.

Calculated ($C_{18}H_{11}N_5O_2 \cdot 0.5H_2O$): C, 63.90; H, 3.58; N, 20.70%. Found: C, 63.84; H, 3.39; N, 20.78%.

HRMS: calculated m/z for $C_{18}H_{11}N_5O_2$: $(M + H)^+$ 330.0986. Found: $(M + H)^+$ 330.0997.

IR (KBr, cm^{-1}): 3424 [w. br], 3047.77 [w. br] 1723 [s. sh], 1635 [s. sh], 1576 [w. sh], 1557 [w. sh], 1509 [s.

br], 1445 [w], 1407 [m], 1223 [s. sh], 1180 [s. sh], 1064 [s. sh], 1011 [s. sh], 752 [m. sh], 686 [m. sh].

^{1}H NMR (d^6-DMSO, 500 MHz): **δ** 15.13 (s, 1H, O–**H**N), 9.11 (dd, *J* = 4.5, 1.7 Hz, 1H, Phen**H**), 8.94 (dd, *J* = 4.4, 1.6 Hz, 2H, Py**H**), 8.90 (dd, *J* = 4.5, 1.7 Hz, 1H, Phen**H**), 8.61 (dd, *J* = 7.9, 1.7 Hz, 1H, Phen**H**), 8.50 (d, *J* = 7.9 Hz, 1H, Phen**H**), 7.88 (dd, *J* = 4.4, 1.6 Hz, 2H, Py**H**), 7.75 (dd, *J* = 7.9, 4.5 Hz, 1H, Phen**H**), 7.67 (dd, *J* = 7.9, 4.5 Hz, 1H, Phen**H**).

^{13}C NMR (d^6-DMSO, 125 MHz): **δ** 181.9 (Phen**C**=O), 164.5 (**C**=O), 156.2 (Phen**C**), 152.7 (Phen**C**), 151.6 (Phen**C**), 151.4(Pyr**C**), 147.1 (Phen**C**), 139.4 (Pyr**C**), 136.3 (Phen**C**), 135.1 (Phen**C**), 132.2 (Phen**C**), 128.6 (Phen**C**), 127.8 (Phen**C**), 125.6 (Phen**C**), 125.3 (Phen**C**), 122.0 (Pyr**C**).

*[Ag(**1**)$_2$]NO$_3$ and [Ag(**1**)$_2$]BF$_4$*

A solution of $AgNO_3$ or $AgBF_4$ (0.085 g or 0.097 g, respectively, 0.500 mmol) in MeCN (20 cm^3) was added to a warm solution of **1** (0.329 g, 1.00 mmol) in MeCN (80 cm^3). The resulting suspension was refluxed for 3 h and filtered whilst hot to give an orange/yellow solid. The solid was washed with hot MeCN (3 × 20 cm^3) and then with hot DCM (5 × 20 cm^3), and dried under vacuum.

[Ag(**1**)$_2$]NO$_3$·2H$_2$O yield: 0.316 g, 76%.

Calculated $[Ag(C_{18}H_{11}N_5O_2)_2]NO_3{\cdot}2H_2O$: C, 50.01; H,3.03; N, 17.82%. Found: C, 50.44; H, 2.79; N, 17.91%.

MS: calculated *m/z* for $[Ag(C_{18}H_{11}N_5O_2)_2]^+$: $(M)^+$ 765.0876. Found: $(M)^+$ 765.0873.

IR (KBr, cm^{-1}): 3412 [w. br], 3078 [w. br], 1712 [s. sh], 1631 [s. sh], 1578 [w. sh], 1564 [w. sh], 1510 [s. br], 1455 [w], 1409 [m], 1340 [s. br], 1217 [s. sh], 1187 [s. sh], 1068 [s. sh], 1048 [m. sh], 1020 [s. sh], 844 [w. sh], 830 [w. sh], 749 [w. sh], 679 [m. sh], 633 [w. sh].

^{1}H NMR (d^6-DMSO, 500 MHz): **δ** 15.15 (s, 2H, O–**H**N), 9.14 (dd, *J* = 4.8, 1.7 Hz, 2H, Phen**H**), 8.97-8.93 (m, 6H, 2Phen**H** & 4Py**H**), 8.84 (dd, *J* = 8.0, 1.7 Hz, 2H, Phen**H**), 8.73 (d, *J* = 8.0 Hz, 2H, Phen**H**), 7.98 (dd, *J* = 8.0, 4.8 Hz, 2H, Phen**H**), 7.93-7.90 (m, 6H, 2Phen**H** & 4Py**H**).

^{13}C NMR (d^6-DMSO, 125 MHz): **δ** 180.9 (Phen**C** = O), 164.5 (**C** = O), 156.4 (Phen**C**), 152.2 (Phen**C**), 151.5 (Pyr**C**), 149.6 (Phen**C**), 144.1 (Phen**C**), 139.3 (Pyr**C**), 137.9 (Phen**C**), 134.7 (Phen**C**), 134.0 (Phen**C**), 130.1 (Phen**C**), 128.9 (Phen**C**), 127.3 (Phen**C**), 126.9 (Phen**C**), 122.1 (Pyr**C**).

[Ag(**1**)$_2$]BF$_4$ Yield: 0.305 g, 72%.

Calculated $[Ag(C_{18}H_{11}N_5O_2)_2]BF_4$: C, 50.67; H, 2.60; N, 16.41%. Found: C, 50.02; H, 2.24; N, 16.06%.

MS: Calculated *m/z* for $[Ag(C_{18}H_{11}N_5O_2)_2]^+$: $(M)^+$ 765.0876. Found: $(M)^+$ 765.0908;

IR (KBr, cm^{-1}): 3402 [w. br], 3101 [w. br], 1706 [s. sh], 1629 [m. sh], 1580 [w. sh], 1564 [w. sh], 1521 [s. br], 1458 [w], 1409 [s, sh], 1290 [w. sh], 1228 [m. sh], 1185 [m. sh], 1080–1030 [s. br *ν*(BF_4)], 1021 [s. sh], 846 [w. sh], 816 [w. sh], 747 [w. sh], 681 [m. sh], 631 [w. sh].

^{1}H NMR (d^6-DMSO, 500 MHz): **δ** 15.14 (s, 2H, O–**H**N), 9.13 (dd, *J* = 4.8, 1.7 Hz, 1H, 2Phen**H**), 8.95–8.92 (m, 6H, 2Phen**H** & 4Py**H**), 8.82 (dd, *J* = 8.0, 1.7 Hz, 2H, Phen**H**), 8.70 (d, *J* = 8.0 Hz, 2H, Phen**H**), 7.97 (dd, *J* = 8.0, 4.8 Hz, 2H, Phen**H**), 7.94–7.83 (m, 6H, 2Phen**H** & 4Py**H**).

^{13}C NMR (d^6-DMSO, 125 MHz): **δ** 180.5 (Phen**C**=O), 164.5 (**C**=O), 156.0 (Phen**C**), 151.8 (Phen**C**), 151.1 (Pyr**C**), 149.2 (Phen**C**), 143.6 (Phen**C**), 138.8 (Pyr**C**), 137.5 (Phen**C**), 134.2 (Phen**C**N), 133.5 (Phen**C**), 129.6 (Phen**C**), 128.3 (Phen**C**), 126.9 (Phen**C**), 126.5 (Phen**C**), 121.6 (Pyr**C**).

Slow diffusion of DCM vapour into a saturated DMSO solution of [Ag(**1**)$_2$]NO$_3$·2H$_2$O over a period of 9 months resulted in the formation of yellow crystals of $\{[Ag(\mathbf{1})(NO_3)]\}_n$ which were suitable for X-ray crystallographic analysis.

*[Mn(**1**)$_2$](NO$_3$)$_2$·2H$_2$O*

A solution of $Mn(NO_3)_2{\cdot}4H_2O$ (0.126 g, 0.500 mmol) in MeCN (20 cm^3) was added to a warm solution of **1** (0.329 g, 1.000 mmol) in MeCN (80 cm^3) and the bright yellow suspension refluxed for 3 h. The mixture was filtered whilst hot and the orange solid washed with hot MeCN (3 × 20 cm^3) and then hot dichloromethane (5 × 20 cm^3), and dried under vacuum.

Yield: 0.310 g, 70%.

Calculated $[Mn(C_{18}H_{11}N_5O_2)_2](NO_3)_2{\cdot}2H_2O$: C, 49.50; H, 3.00; N, 19.24%. Found: C, 49.67; H, 2.45; N, 19.02%.

IR (KBr, cm^{-1}): 3422 [w. br], 3091 [w. br], 1719 [s. sh], 1642 [s. sh], 1575 [m. sh], 1520 [s. br], 1443 [s. br], 1421 [s. sh], 1385 [s. sh], 1303 [s. br], 1265 [m. sh], 1225 [s. sh], 1186 [m. sh], 1071 [m. sh], 1020 [s.

sh], 844 [w. sh], 819 [w. sh], 748 [m. sh], 682 [m. sh], 639 [w. sh].

μ_{eff} = 6.2 B.M.

Biological testing

Antibacterial activity

The antibacterial susceptibility profiles of Gram-positive *S. aureus* (ATCC 25923) and Gram-negative *P. aeruginosa* (ATCC 27853) were determined according to the protocol recommended by the Clinical and Laboratory Standards Institute (CLSI) (CLSI 2012a, b) using a 96-well microtiter plate with Mueller–Hinton broth (MHB) containing different concentrations of each test compound (starting from a 20 mM solution in DMSO) and classical antibacterial agents (ciprofloxacin and ceftazidime). The lowest concentration of each compound that inhibited bacterial growth, as ascertained by the absence of visible turbidity in each well, was considered to be the MIC value.

Anti-mycobacterial activity

Activities of the test compounds as well as isoniazid were assessed against *M. tuberculosis* $H_{37}Rv$ (ATCC 27294) using the microplate Alamar Blue Assay (Accumed International, Westlake, OH, USA) (Franzblau et al. 1998). This methodology is nontoxic, uses a thermally-stable reagent and shows good correlation with proportional and BACTEC radiometric methods (Tortoli et al. 2002; Kontos et al. 2004). Mycobacteria were grown in Middlebrook 7H9 medium (Becton–Dickinson, Sparks, MD, USA) supplemented with 10% oleic acid-albumin-dextrose-catalase (OADC) and 0.05% Tween 80 and on Middlebrook 7H10 solid agar medium (Becton–Dickinson) supplemented with 10% OADC. The MICs were determined as described previously (Franzblau et al. 1998). Briefly, all mycobacterial strains were prepared from scoops of solid culture and suspended in PBS plus Tween 80, to reach a concentration equivalent to McFarland Standard No. 1 (approximately 3×10^7 colony-forming units (CFU)/mL) and then diluted in Middlebrook 7H9 medium supplemented with 10% OADC to about 10^5 CFU/mL. One hundred microliters of the bacterial suspensions were added to microtiter plates containing, in each well, twofold diluted drugs in 100 µL of Middlebrook 7H9 medium with 10% OADC. The volume of drug-free and mycobacteria-free wells was adjusted to 200 µL and used as the control. The plates were incubated at 37 °C for 5 days. Twenty microliters of Alamar Blue dye and 12.5 µL of 20% sterilized Tween 80 reagent were added. The plates were re-incubated at 37 °C for 24 h, and the colors of all wells were recorded. The MIC was defined as the lowest drug concentration that prevented a color change from blue to pink.

Antifungal activity

Antifungal susceptibility testing was performed using *Candida albicans* (ATCC 36802) according to the standardized broth microdilution technique described by the CLSI (CLSI 2008) and was interpreted according to the CLSI published document (CLSI 2012a, b). The test compounds and the clinical antifungal drug, amphotericin B, were evaluated and the MICs were determined by visual inspection following incubation in a humid atmosphere at 35 °C for 48 h.

Cytotoxicity assay

The effects of the test compounds on the viability of A549 cells (ATCC CCL-185, alveolar basal epithelial cell of human adenocarcinoma) was evaluated using the MTT assay (Mosmann 1983). First, the A549 cells were allowed to adhere in 96-well tissue culture plates, and then the cells were treated with increasing concentrations of the compounds and incubated up to 48 h at 37 °C in a 5% CO_2 atmosphere. Subsequently, the culture medium was discarded and the formation of formazan crystals was measured by adding MTT (5 mg/mL in PBS, 25 µg/mL) and incubating the wells for an additional 3 h in the dark at 37 °C. The plates were centrifuged at $500 \times g$ for 10 min, the supernatant removed, the pellet dissolved in 200 µL of DMSO and the absorbance measured in an ELISA reader at 570 nm (SpectraMax Gemini 190, Molecular Devices, CA, USA). The 50% cytotoxicity inhibitory concentration (CC_{50}) was determined by linear regression analysis.

Results and discussion

Chemical synthesis

The hydrazide ligand **1** was prepared in good yield using a Schiff base condensation reaction between INH and phendione under acidic conditions. Although our initial aim was to carry out a Schiff base reaction at both carbonyl groups of phendione (by treatment with two equivalents of INH) only the mono Schiff base hydrazide formed. Even in the presence of a large excess INH (up to four equivalents) the double Schiff base adduct was not isolated. In this context, our group has previously reported that not all intended double Schiff base reactions proceed as anticipated upon reaction of phendione with amines. For example, chiral, multi-ring products formed upon reaction of phendione with *N,N'*-bis(2-aminophenyl)ethylenediamine (Coyle et al. 2003) and diethylenetriamine (Lin et al. 2006). Also, combining phendione with urea produced bipyridine-glycoluril (Elmans et al. 1998) whilst the reaction with L-tyrosine methyl ester gave a novel phenanthroline-oxazine (McCann et al. 2013).

Whereas the IR spectrum of phendione contains a ν(C=O) band at 1685 cm^{-1} the spectrum of **1** has the carbonyl stretching band at 1723 cm^{-1} and an imine C=N stretch at 1635 cm^{-1} (Supplementary Material). The ^{1}H NMR spectrum of **1** (d^6-DMSO) (Supplementary material) showed an uncharacteristic downfield resonance for the amide H atom at 15.08 ppm, suggesting that H-bonding is taking place between it and the O atom of the ketone group on the backbone of the phendione moiety. H-bonding of this type has previously been documented for hydrazones of similar structure and it leads to keto-enol tautomerization (Benković et al. 2018; Cheon et al. 2002; Barbazán et al. 2010). The ^{1}H NMR spectrum of **1** in d^4-methanol shows additional peaks in the region 7.5–9.1 ppm compared to that recorded in d^6-DMSO, indicating that the tautomerization process is more clearly observed in the former solvent. It is believed that it is the presence of the intramolecular H-bonding between the NH moiety of the hydrazone and ketone oxygen atom which causes the carbonyl carbon to be less electrophilic and thus decreases the susceptibility of this carbonyl group toward further Schiff base (imine) formation. Imine functionalities are well known to undergo hydrolysis back to starting materials (Yildiz 2016; Buss and Ponka 2003). Thus, the stability of **1** towards hydrolysis was investigated by monitoring changes in the ^{1}H NMR spectrum of a solution of the compound in d^6-DMSO upon addition of a few drops of D_2O. No spectral changes were observed over a period of 1 week at ambient temperature indicating the relative stability of the C=N moiety towards hydrolysis. The structure of **1** is expected to be essentially identical to that of the closely related hydrazones formed by reacting phendione with benzoic acid hydrazide and 2-hydroxybenzoic acid hydrazide (Barbazán et al. 2010).

Metal complexes of **1** were synthesised by reacting simple Ag^+ and Mn^{2+} tetrafluoroborate or nitrate salts with ligand **1** in a metal ion:ligand ratio of 1:2. The resulting complexes formulated as $[Ag(\mathbf{1})_2]NO_3$, $[Ag(\mathbf{1})_2]BF_4$ and $[Mn(\mathbf{1})_2](NO_3)_2$. The IR spectra of the complexes contained bands associated with ligand **1** and the NO_3^-/BF_4^- anions (Supplementary material). The mass spectra of the Ag^+ complexes showed peaks for the $[Ag(\mathbf{1})_2]^+$ ion with characteristic isotopic patterns (Supplementary Material). Small shifts of the signals for the phenanthroline protons are seen when the ^{1}H NMR spectrum (d^4-methanol) of the free ligand is compared to those of the Ag^+ complexes. It is anticipated that in the core structure of the Ag^+ and Mn^{2+} complexes the metal ion is chelated by both nitrogen atoms from the phendione moiety of each molecule of **1**, as has been shown previously in the cases of $[Ag(phendione)_2]ClO_4$ (McCann et al. 2004), $[Ag(phendione)(CH_3CO_2)]\cdot 3H_2O$ (Oneugbu et al. 2008) and $[Cu(phendione)_3](ClO_4)_2\cdot 2H_2O\cdot 2MeCN$ (Liu et al. 2000). Intermolecular coordination by the pyridine N atom of the INH moiety of **1** is also possible.

Interestingly, when the ^{1}H NMR spectrum of $[Ag(\mathbf{1})_2]NO_3\cdot 2H_2O$ was recorded in d^6-DMSO new peaks appeared over a period of 3 days (Supplementary Material), the solution colour darkened visibly and precipitation was observed. These effects occurred both in the presence and in the absence of light but were not seen with the $[Ag(\mathbf{1})_2]BF_4$ sample (NMR spectrum remained unchanged and the solution did not darken in the presence of light). Furthermore, slow diffusion of DCM vapour into a saturated DMSO solution of $[Ag(\mathbf{1})_2]NO_3\cdot 2H_2O$ over a prolonged period resulted in the formation of a new complex which X-ray crystallographic analysis revealed it to be polymeric and formulating with the 1:1 metal:ligand stoichiometry, $\{[Ag(\mathbf{1})(NO_3)]\}_n$ (Figs. 1, 2, 3;

Table 2). In this complex, ligand **1** is seen to be ambidentate. Each Ag^{+} ion is bonded to three heterocyclic nitrogen atoms with the shortest Ag–N distance to the pyridine N atom of the INH moiety (Ag1–N1; 2.225(3) Å) and there are longer bonds to the *N,N'* chelating atoms of the phendione moiety of the adjacent ligand molecule (Ag1–$N16^{i}$ and Ag1–$N19^{i}$; 2.434(3) and 2.314(3) Å, respectively; i = equivalent atom symmetry generation transformation x − 1, y + 1, z − 1). The chelating phendione moiety creates the narrowest N–Ag–N angle ($N19^{i}$–Ag1–$N16^{i}$; 70.24(10)°), whilst N1–Ag1–$N16^{i}$ is 118.56(10)°. The N1–Ag1–$N19^{i}$ angle of 163.08(10)° is closest to being linear. The nitrate anion chelates to the central Ag^{+} ion (Ag–O28; 2.6468(28) and Ag–O27; 2.7822(27) Å), and it also serves to link the polymeric planes via extensive hydrogen bonding (Fig. 3). Finally, there is an intramolecular hydrogen bond within ligand **1** involving the hydrogen attached to N9 of the INH moiety and the carbonyl oxygen (O25) of the phendione moiety (Figs. 1, 2). The existence of such an intramolecular hydrogen bond within the metal-free ligand **1** was

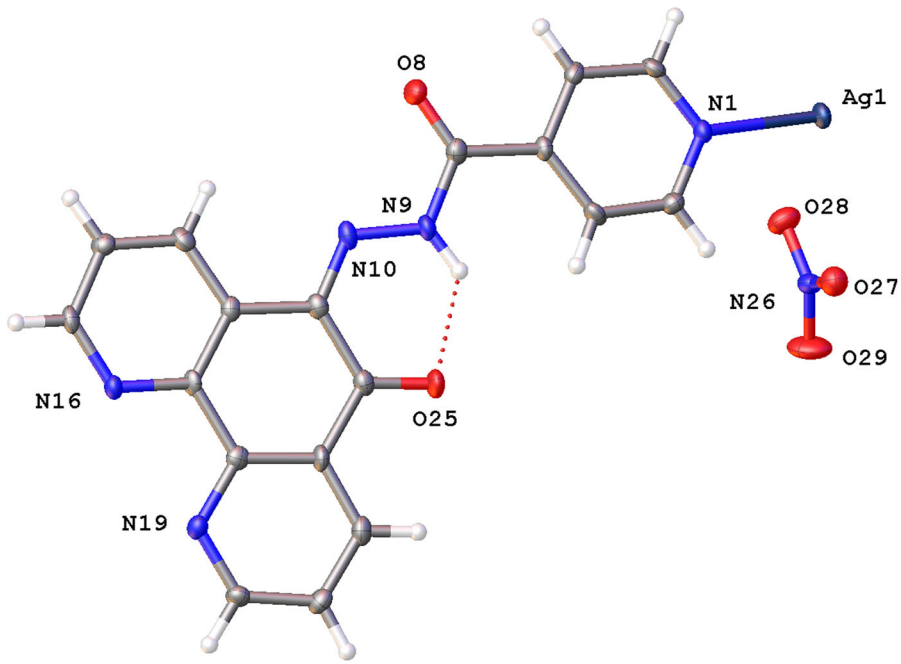

Fig. 1 Asymmetric unit of $\{[Ag(\mathbf{1})(NO_3)]\}_n$ with selected atom numbering. Atomic displacement shown at 50% probability. Intramolecular hydrogen bonding shown as a dotted line

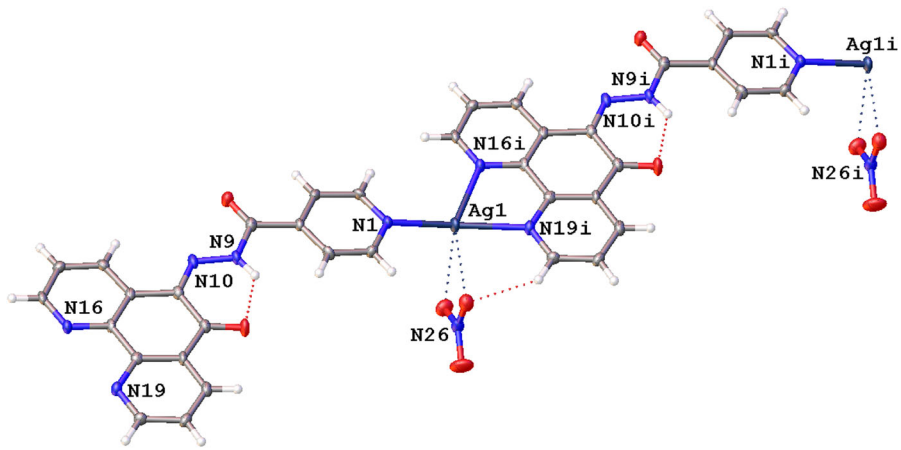

Fig. 2 Symmetry generated (symmetry code used to generate equivalent atoms i = x − 1, y + 1, z − 1) chain for $\{[Ag(\mathbf{1})(NO_3)]\}_n$ with intramolecular hydrogen bonding showing the Ag^{+} coordination by the nitrate anion

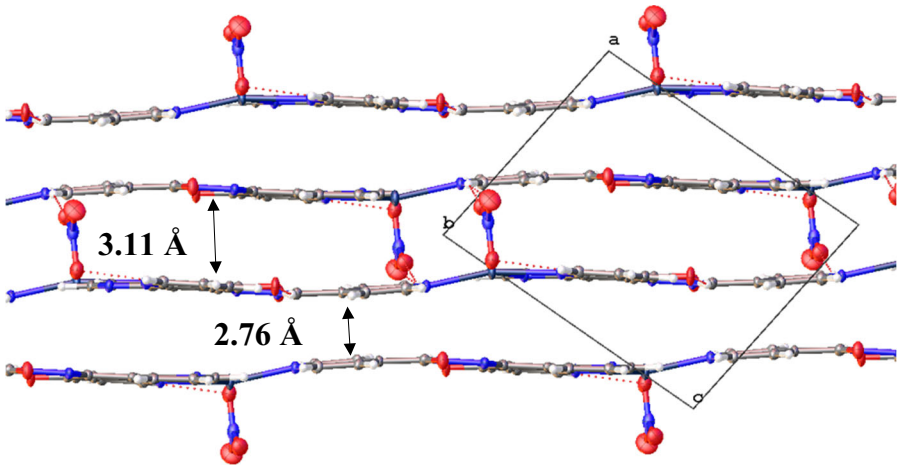

Fig. 3 Lamellar arrangement of $\{[Ag(\mathbf{1})_2(NO_3)]\}_n$ viewed normal to the b-axis. The average distances between the planes described by the atoms in the ligand are ca. (a) 3.11 Å between the two planes incorporating the nitrate anion via hydrogen bonding and (b) 2.76 Å separating these hydrogen bonded dimeric planes

inferred earlier from the ^{1}H NMR spectral studies of metal-free **1**.

Biological studies

The results of the biological screening studies for the metal-free ligand, **1**, the Ag^+ and Mn^{2+} complexes of **1**, metal-free 1,10-phenanthroline, simple metal salts and some clinically used drugs are compiled in Tables 3 and 4.

Anti-*M. tuberculosis* activity

In terms of μM concentrations, the metal-free ligands, **1** and 1,10-phenanthroline, showed very similar activities against *M. tuberculosis* strain $H_{37}RV$ (Table 3), suggesting that the INH moiety of **1** is not playing a dominant role in inhibiting the growth of this bacterium. Furthermore, these two metal-free ligands were only marginally less effective than the prescribed drug, isoniazid. Whilst the simple metal salts, $AgBF_4$ and $Mn(NO_3)_2{\cdot}4H_2O$, displayed only marginal (Ag^+) to poor (Mn^{2+}) activities, the metal complexes of **1**, $[Ag(\mathbf{1})_2]BF_4$, $[Ag(\mathbf{1})_2]NO_3{\cdot}2H_2O$ and $[Mn(\mathbf{1})_2](NO_3)_2{\cdot}2H_2O$, were almost fourfold more potent than isoniazid. Interestingly, there was no real variation in activity across the three members of the group of metal complexes of **1**, suggesting that activity was independent of the type of chelated central metal ion (Ag^+ or Mn^{2+}). This is in stark contrast to the trend observed with the simple metal salts where the performance of $AgBF_4$ was over 11-fold superior to $Mn(NO_3)_2{\cdot}4H_2O$. It was also evident that the potencies of the three metal complexes of **1** were significantly better than the combined activities of metal-free **1** and its respective simple metal salt, implying that dispensing the complex as a discrete entity was appreciably more beneficial than the additive effect of administering separate units of metal-free **1** along with the simple metal salt.

Encouragingly, preliminary tests involving three different rifampicin- and isoniazid-resistant *M. tuberculosis* strains (665/0514, SR Cult 84/17 and SR

Table 2 Selected bond lengths [Å] and angles [°] for $\{[Ag(\mathbf{1})(NO_3)]\}_n$

Ag1–N1	2.225(3)
Ag1–N16^i	2.434(3)
Ag1–N19^i	2.314(3)
O8–C7	1.212(4)
O25–C24	1.230(4)
N1–C2	1.336(4)
N1–C6	1.347(5)
N9–N10	1.347(4)
N9–C7	1.386(5)
N9–H9	0.899(10)
N1–Ag1–N16^i	118.56(10)
N1–Ag1–N19^i	163.08(10)
N19^i–Ag1–N16^i	70.24(10)

Symmetry transformations used to generate equivalent atoms: i = x − 1, y + 1, z − 1

Table 3 Effects of test compounds on some clinically relevant microorganisms

Compounds	MIC (μg/ml (μM))			
	M. tuberculosis $H_{37}Rv$ (ATCC 27294)[a]	*S. aureus* (ATCC 25923)	*P. aeruginosa* (ATCC 27853)	*C. albicans* (ATCC 36802)
1	5 (15.18)	16 (48.59)	128 (388.69)	4 (12.15)
$[Ag(\mathbf{1})_2]BF_4$	2.5 (2.93)	8 (9.38)	8 (9.38)	2 (2.34)
$[Ag(\mathbf{1})_2]NO_3{\cdot}2H_2O$	2.5 (2.89)	16 (18.51)	8 (9.25)	2 (2.31)
$[Mn(\mathbf{1})_2](NO_3)_2{\cdot}2H_2O$	2.5 (2.99)	16 (19.10)	512 (611.29)	16 (19.10)
$AgBF_4$	10 (51.36)	4 (20.54)	2 (10.27)	0.25 (1.29)
$Mn(NO_3)_2{\cdot}4H_2O$	> 100 (> 558.82)	64 (355.14)	64 (355.14)	> 512 (> 2861.13)
1,10-Phenanthroline	2.5 (13.87)	> 512 (> 2861.13)	> 512 (> 2861.13)	0.25 (1.39)
Isoniazid	1.56 (11.38)	ND	ND	ND
Amphotericin B	ND	ND	ND	0.06 (0.06)
Ciprofloxacin	ND	4 (12.07)	4 (12.07)	ND
Ceftazidime	ND	16 (29.28)	4 (7.32)	ND

ND non-determined

[a]Rifampicin- and isoniazid-sensitive strain

Table 4 Toxicity of test compounds on A549 epithelial cells and selectivity index (SI) values for the test microorganisms

Compounds	CC_{50}, μM	Selectivity index (SI)[a] values			
	A549 epithelial cells	*M. tuberculosis* $H_{37}Rv$ (ATCC 27294)	*S. aureus* (ATCC 25923)	*P. aeruginosa* (ATCC 27853)	*C. albicans* (ATCC 36802)
1	157.23	10.36	3.24	0.40	12.94
$[Ag(\mathbf{1})_2]BF_4$	44.11	15.05	4.70	4.70	18.85
$[Ag(\mathbf{1})_2]NO_3{\cdot}2H_2O$	48.47	16.76	2.62	5.24	21.01
$[Mn(\mathbf{1})_2](NO_3)_2{\cdot}2H_2O$	56.67	18.95	2.97	0.09	2.97
$AgBF_4$	95.53	1.86	4.65	9.30	74.05
1,10-Phenanthroline	2422.29	174.64	6.82	6.82	1742.65
Isoniazid	3500.10	307.57	ND	ND	ND
Amphotericin B	8.59	ND	ND	ND	143.17

ND non-determined

[a]SI = CC_{50} value/MIC value

2571/0215) have revealed that **1** and its Ag^+ and Mn^{2+} complexes greatly impede the growth of these highly resilient bacteria as similarly detected against the sensitive strain, $H_{37}RV$ (data not shown).

Anti-*S. aureus* and *P. aeruginosa* activity

Metal-free **1** and its metal complexes were up to sixfold less active against Gram-positive *S. aureus* in comparison to *M. tuberculosis* (Table 3). In contrast to the observation of the similar activities of metal-free **1** and metal-free 1,10-phenanthroline towards *M. tuberculosis*, the latter ligand was ca. 60-fold less potent than **1** against *S. aureus*, implying that the INH moiety of **1** is exerting a very influential and positive effect on its activity against this bacterium.

S. aureus was more sensitive to $AgBF_4$ and $Mn(NO_3)_2{\cdot}4H_2O$ than *M. tuberculosis*, with the Ag^+ simple salt being the most effective. $[Ag(\mathbf{1})_2]BF_4$, $[Ag(\mathbf{1})_2]NO_3{\cdot}2H_2O$ and $[Mn(\mathbf{1})_2](NO_3)_2{\cdot}2H_2O$ had activities similar to those of the clinical drugs, ciprofloxacin and ceftazidime, the remaining compounds being much less effective.

Metal-free **1** and $[Mn(\mathbf{1})_2](NO_3)_2{\cdot}2H_2O$ were notably much less effective towards Gram-negative *P. aeruginosa* than against *M. tuberculosis* and Gram-positive *S. aureus*. Only $[Ag(\mathbf{1})_2]BF_4$ and $[Ag(\mathbf{1})_2]$-$NO_3{\cdot}2H_2O$ had efficiencies approaching those of ciprofloxacin and ceftazidime towards *P. aeruginosa*.

Anti-*C. albicans* activity

With the exception of the Mn^{2+} simple salt, $Mn(NO_3)_2{\cdot}4H_2O$, all of the test compounds were very active against the fungus, *C. albicans*. Although the compounds were much less effective than the clinical drug, amphotericin B (MIC 0.06 μM), the latter polyene is reputed to have severe nephrotoxicity associated with it which often prompts a discontinuation of therapy despite a life-threatening, systemic fungal infection (Sabra and Branch 1990).

Toxicity versus A549 cell line

Mammalian A549 cells were the least sensitive to metal-free isoniazid, followed by metal-free 1,10-phenanthroline (Table 4). In comparison, metal-free **1**, which is a molecule whose framework is essentially a fusion of isoniazid with 1,10-phenanthroline, was much less well tolerated by the A549 cells. The Ag^+ and Mn^{2+} complexes of **1** were ca. threefold more toxic towards these cells than metal-free **1**. Amphotericin B had the most detrimental effect on the A549 cells.

With respect to *M. tuberculosis* $H_{37}RV$, isoniazid and metal-free 1,10-phenanthroline had the largest calculated Selectivity Index (SI) values (Table 4). Although metal-free **1** and its metal complexes had considerably lower SI values they still fell within the acceptable range (> 10) (Nguta et al. 2015).

With the exception of $AgBF_4$, the SI values for both *S. aureus* and *P. aeruginosa* were very much lower than those found for *M. tuberculosis* $H_{37}RV$ across the range of test compounds (no value > 10). Against the fungus, *C. albicans*, metal-free 1,10-phenanthroline returned an extremely large SI value (1742) and this was followed by amphotericin B (143) and the simple metal salt, $AgBF_4$ (74). Metal-free **1** and its two Ag^+ complexes had SI values in the range 13–21, with the Mn^{2+} complex giving the lowest value (ca. 3).

Finally, it is noteworthy that the core structure of ligand **1** is identical to that of the naturally occurring

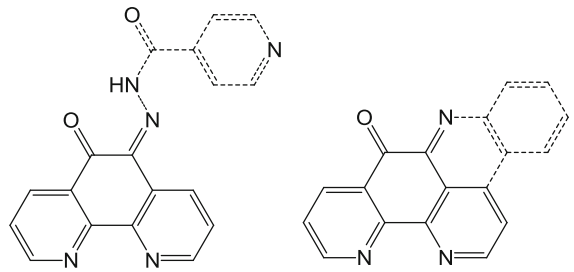

1 **ascididemin**

Fig. 4 Comparison of the core structures (shown in solid bonds) of **1** and ascididemin

marine alkaloid, ascididemin (Fig. 4), which is known to display potent antimicrobial (Bhakuni and Rawat 2010; Lindsay et al. 1995) and antitumor (Delfourne and Bastide 2003; Matsumoto et al. 2003) activity in its metal-free form. It is interesting that metal-free **1** and ascididemin (Lindsay et al. 1995) were both relatively inactive against Gram-negative *P. aeruginosa*. Contrastingly, whereas the current synthetic compounds are somewhat non-toxic towards human lung epithelium A549 cells (CC_{50} = 157.23 μM) these cells are quite intolerant of the pyridoacridine alkaloid (IC_{50} = 0.02 μM) Delfourne and Bastide 2003).

Conclusions

Ligand **1** and its Ag^+ and Mn^{2+} complexes are readily obtained with robust yields from relatively cheap starting materials. Ligand **1** is not susceptible to immediate hydrolysis in presence of H_2O over a period of 7 days and the stability of the Ag^+ complexes varies with the nature of the counterion. The $[Ag(\mathbf{1})_2]NO_3$ complex shows signs of decomposistion with 12 h in a DMSO solution, whereas the $[Ag(\mathbf{1})_2]BF_4$ complex does not display instability in similar conditions when tested over 3 days. The activity displayed by ligand **1** is comparable to **INH** towards *M. tuberculosis* $H_{37}RV$ with its Ag^+ and Mn^{2+} complexes being four times more active. These compounds are more selective towards *M. tuberculosis* $H_{37}RV$ over mammalian A549 cells and display SI vales > 10. In addition, these compounds have very good, broad-spectrum antimicrobial activity.

Supplementary information

Crystallographic data, CCDC 1907353 can be obtained free of charge from the Cambridge Crystallographic Data Centre via www.ccdc.cam.ac.uk/data_request/cif. Electronic supplementary material available.

Acknowledgments We gratefully acknowledge Maynooth University John and Pat Hume Scholarship Award for MA. We also gratefully acknowledge the financial support for the biological studies from the Brazilian agencies CNPq, FAPERJ and CAPES.

References

Barbazán P, Hagenbach A, Oehlke E, Abram U, Carballo R, Rodríguez-Hermida S, Vázquez-López EM (2010) Tricarbonyl rhenium(I) and technetium(I) complexes with hydrazones derived from 4,5-diazafluoren-9-one and 1,10-phenanthroline-5,6-dione. Eur J Inorg Chem 29:4622–4630. https://doi.org/10.1002/ejic.201000522

Benković T, Kenđel A, Parlov-Vuković J, Kontrec D, Chiş V, Miljanić S, Galić N (2018) Aromatic hydrazones derived from nicotinic acid hydrazide as fluorimetric pH sensing molecules: structural analysis by computational and spectroscopic methods in solid phase and in solution. Spectrochim Acta A 190:259–267. https://doi.org/10.1016/j.saa.2017.09.038

Bhakuni DS, Rawat DS (2010) Bioactive marine natural products. Springer, New York, pp 235–277 **(Chapter 9)**

Bruker (2014–2015). SADABS, Bruker AXS Inc., Madison, Wisconsin, USA

Bruker (2015). APEX3 v2015.9-0, Bruker AXS Inc., Madison, WI, USA

Buss JL, Ponka P (2003) Hydrolysis of pyridoxal isonicotinoyl hydrazone and its analogues. Biochim Biophys Acta Gen Subj 1619:177–186. https://doi.org/10.1016/S0304-4165(02)00478-6

Butler HM, Hurse A, Thursky E, Shulman A (1969) Bactericidal action of selected phenanthroline chelates and related compounds. Aust J Exp Biol Med Sci 47:541–552

Butler HM, Laver JC, Shulman A, Wright RD (1970) The use of phenanthroline metal chelates for the control of topical infections due to bacteria, fungi and protozoa. Med J Aust 2:309–314. https://doi.org/10.5694/j.1326-5377.1970.tb50012.x

Cade G, Shankly KH, Shulman A, Wright RD, Stahle IO, Macgibbon CB, Lew-Sang E (1970) The treatment of dermatological infections with a manganese phenanthroline chelate—a controlled clinical trial. Med J Aust 2:304–309. https://doi.org/10.5694/j.1326-5377.1970.tb50011.x

Cheon K-S, Park YS, Kazmaier PM, Buncel E (2002) Studies of azo–hydrazone tautomerism and H-bonding in azo-functionalized dendrimers and model compounds. Dyes Pigm 53:3–14. https://doi.org/10.1016/S0143-7208(01)00096-1

Clinical and Laboratory Standards Institute (CLSI) (2008) Reference method for broth dilution antifungal susceptibility testing of yeasts. Approved Standard-Third Edition. CLSI Document M-27A3, CLSI, Wayne, PA, USA

Clinical and Laboratory Standards Institute (CLSI) (2012a) Methods for dilution antimicrobial susceptibility tests for bacteria that grow aerobically: M07-A9. CLSI, Wayne, PA, USA

Clinical and Laboratory Standards Institute (CLSI) (2012b) Reference method for broth dilution antifungal susceptibility testing of yeasts. Fourth Informational Supplement. CLSI Document M27-S4, CLSI, Wayne, PA, USA

Coyle B, McCann M, McKee V, Devereux M (2003) Synthesis and X-ray crystal structure of a tetracyclic gem-cis-bis(aminal) formed from N, N'-bis(2-aminophenyl)ethylenediamine and 1,10-phenanthroline-5,6-dione. ARKIVOC 7(7):59–66. https://doi.org/10.3998/ark.5550190.0004.707

Delfourne E, Bastide J (2003) Marine pyridoacridine alkaloids and synthetic analogues as antitumor agents. Med Res Rev 23:234–252. https://doi.org/10.1002/med.10032

Dolomanov OV, Bourhis LJ, Gildea RJ, Howard JAK, Puschmann HJ (2009) OLEX2: a complete structure solution, refinement and analysis program. Appl Cryst 42:339–341. https://doi.org/10.1107/S0021889808042726

Dwyer FP, Gyarfas EC, Wright RD, Shulman A (1957) Effect of inorganic complex ions on transmission at a neuromuscular junction. Nature 179:425–426

Dwyer FP, Reid IK, Shulman A, Laycock GM, Dixson S (1969a) Biological actions of 1,10-phenanthroline and 2,2′-bipyridine hydrochloride, quaternary salts, and metal chelates and related compounds. I. Bacteriostatic action on selected gram-positive, gram-negative, and acid-fast bacteria. Aust J expt Biol Med Sci 47:203–218. https://doi.org/10.1038/icb.1969.21

Dwyer FP, Wright RD, Shulman A (1969) Animal and plant therapeutic compositions, Canadian Patent No. 824,652

Elmans JAAW, Gelder R, Rowan AE, Nolte RJM (1998) Bipyridine functionalized molecular clips. Self-assembly of their ruthenium complexes in water. Chem Commun 45:1553–1554. https://doi.org/10.1039/A803327G

Franzblau SG, Witzig RS, McLaughlin JC, Torres P, Madico G, Hernandez A, Degnan MT, Cook MB, Quenzer VK, Ferguson RM, Gilman RH (1998) Rapid, low-technology MIC determination with clinical *Mycobacterium tuberculosis* isolates by using the microplate Alamar Blue assay. J Clin Microbiol 36:362–366

Kontos F, Maniati M, Costopoulos C, Gitti Z, Nicolaou S, Petinaki E, Anagnostou S, Tselentis I, Maniatis AN (2004) Evaluation of the fully automated Bactec MGIT 960 system for the susceptibility testing of *Mycobacterium tuberculosis* to first-line drugs: a multicenter study. J Microbiol Methods 56:291–294. https://doi.org/10.1016/j.mimet.2003.10.015

Lin L, Qiu YC, Zeng RH, Wu JZ (2006) (1R)-6,9,15,18,21-Pentaazapentacyclo[12.7.0.01,18.02,7.08,13]henicosa-2,4,6,8(13),9,11,14-heptaene. Acta Cryst 62:o3739–o3741. https://doi.org/10.1107/S1600536806030558

Lindsay BS, Borrows LR, Copp BR (1995) Structural requirements for biological activity of the marine alkaloid

ascididemin. Bioorg Med Chem Lett 5:739–742. https://doi.org/10.1016/0960-894X(95)00106-4

Liu H, Du M, Leng X-B, Bu X-H, Zhang R-H (2000) Synthesis and crystal structure of the copper(II) complex with tris-(1,10- phenanthroline-5,6-dione). Chin J Struct Chem 19:427–431

MacLeod RA (1952) The toxicity of o-phenanthroline for lactic acid bacteria. J Biol Chem 197:751–761

Matsumoto SS, Biggs J, Copp BR, Holden JA, Barrows LR (2003) Mechanism of ascididemin-induced cytotoxicity. Chem Res Toxicol 16:113–122. https://doi.org/10.1021/tx025618w

McCann M, Coyle B, McKay S, McCormack P, Kavanagh K, Devereux M, McKee V, Kinsella P, O'Connor R, Clynes M (2004) Synthesis and X-ray crystal structure of $[Ag(phendio)_2]ClO_4$ (phendio = 1,10-phenanthroline-5,6-dione) and its effects on fungal and mammalian cells. Biometals 17:635–654. https://doi.org/10.1007/s10534-004-1229-5

McCann M, Kellett A, Kavanagh K, Devereux M, Santos ALS (2012a) Deciphering the antifungal activity of phenanthroline chelators. Curr Med Chem 19:2703–2714. https://doi.org/10.2174/092986712800609733

McCann M, Santos ALS, da Silva BA, Romanos MTV, Pyrrho AS, Devereux M, Kavanagh K, Fichtner I, Kellett A (2012b) *In vitro* and in vivo studies into the biological activities of 1,10-phenanthroline, 1,10-phenanthroline-5,6-dione and its copper(II) and silver(I) complexes. Toxicol Res 1:47–54. https://doi.org/10.1039/C2TX00010E

McCann M, McGinley J, Ni K, O'Connor M, Kavanagh K, McKee V, Colleran J, Devereux M, Gathergood N, Barron N, Prisecaru A, Kellett A (2013) A new phenanthroline-oxazine ligand: synthesis, coordination chemistry and atypical DNA binding interaction. Chem Commun 49:2341–2343. https://doi.org/10.1039/C3CC38710K

McCarron P, McCann M, Devereux M, Kavanagh K, Skerry C, Karakousis PC, Carolina Aor A, Mello TP, Santos ALS, Campos DL, Pavan FR (2018) Unprecedented in vitro antitubercular activitiy of manganese(II) complexes containing 1,10-phenanthroline and dicarboxylate ligands: increased activity, superior selectivity and lower toxicity in comparison to their copper(II) analogues. Front Microbiol 9:1–10. https://doi.org/10.3389/fmicb.2018.01432

Mosmann T (1983) Rapid colorimetric assay for cellular growth and survival: application to proliferation and cytotoxicity assays. J Immunol Methods 65:55–63. https://doi.org/10.1016/0022-1759(83)90303-4

Nguta JM, Opong AR, Nyarko AK, Manu YD, Addo PGA (2015) Current perspective in drug discovery against tuberculosis from natural products. Int J Mycobacteriol 4:165–183. https://doi.org/10.1016/j.ijmyco.2015.05.004

Oneugbu J, Butcher RJ, Hosten C, Udeochu UC, Bakare O (2008) Acetato(1,10-phenanthroline-5,6-dione)silver(I) trihydrate. Acta Cryst E64:403–404. https://doi.org/10.1107/S1600536808000846

Sabra R, Branch RA (1990) Amphotericin B nephrotoxicity. Drug Saf 5:94–108. https://doi.org/10.2165/00002018-199005020-00003

Seventh World Health Assembly, Improving the prevention, diagnosis and clinical management of sepsis. http://apps.who.int/gb/ebwha/pdf_files/WHA70/A70_R7-en.pdf?ua=1. Accessed 1 Nov 2018

Sheldrick GM (2008) A short history of SHELX. Acta Cryst A64:112–122. https://doi.org/10.1107/S0108767307043930

Sheldrick GM (2015) SHELXT – Integrated space-group and crystal-structure determination. Acta Cryst A71:3–8. https://doi.org/10.1107/S2053273314026370

Shulman A, Dwyer FP (1964) Metal chelates in biological systems. In: Dwyer FP, Mellor DP (eds) Chelating agents and metal chelates. Academic Press, New York

Tortoli E, Benedetti M, Fontanelli A, Simonetti MT (2002) Evaluation of automated BACTEC MGIT 960 system for testing susceptibility of *Mycobacterium tuberculosis* to four major antituberculous drugs: comparison with the radiometric BACTEC 460 TB method and the agar plate method of proportion. J Clin Microbiol 40:607–610. https://doi.org/10.1128/JCM.40.2.607-610.2002

Viganor L, Howe O, McCarron P, McCann M, Devereux M (2017) The antibacterial activity of metal complexes containing 1,10-phenanthroline: potential as alternative therapeutics in the era of antibiotic resistance. Curr Top Med Chem 17:1280–1302. https://doi.org/10.2174/1568026616666161003143333

WHO factsheet sepsis, http://www.who.int/news-room/fact-sheets/detail/sepsis. Accessed 1 Nov 2018

Yildiz IA (2016) A DFT approach to the mechanistic study of hydrozone hydrolysis. J Phys Chem A 120:3683–3692. https://doi.org/10.1021/acs.jpca.6b02882

Zheng RH, Guo HC, Jiang HJ, Xu KH, Liu BB, Sun WL, Shen ZQ (2010) A new and convenient synthesis of phendiones oxidated by KBr O_3/H_2SO_4 at room temperature. Chin Chem Lett 21:1270–1272. https://doi.org/10.1016/j.cclet.2010.05.030